Inorganic Chemistry

ARTICLE

pubs.acs.org/IC

Electronic Properties and ^{13}C NMR Structural Study of $Y_3N@C_{88}$

Wujun Fu, Jianyuan Zhang, Hunter Champion, Tim Fuhrer, Hugo Azuremendi, Tianming Zuo, Jianfei Zhang, Kim Harich, and Harry C. Dorn*

Department of Chemistry, Virginia Polytechnic Institute and State University, Blacksburg, Virginia 24061, United States

Supporting Information

ABSTRACT: In this paper, we report the synthesis, purification, ^{13}C NMR, and other characterization studies of $Y_3N@C_{88}$. The ^{13}C NMR, UV−vis, and chromatographic data suggest an $Y_3N@C_{88}$ having an IPR-allowed cage with $D_2(35)$-C_{88} symmetry. In earlier density functional theory (DFT) computational and X-ray crystallographic studies, it was reported that lanthanide $(A_3N)^{6+}$ clusters are stabilized in $D_2(35)$-C_{88} symmetry cages and have reduced HOMO−LUMO gaps relative to other trimetallic nitride endohedral metallofullerene cage systems, for example, $A_3N@C_{80}$. In this paper, we report that the nonlanthanide $(Y_3N)^{6+}$ cluster in the $D_2(35)$-C_{88} cage exhibits a HOMO−LUMO gap consistent with other lanthanide $A_3N@C_{88}$ molecules based on electrochemical measurements and DFT computational studies. These results suggest that the reduced HOMO−LUMO gap of $A_3N@C_{88}$ systems is a property dominated by the $D_2(35)$-C_{88} carbon cage and not f-orbital lanthanide electronic metal cluster $(A_3N)^{6+}$ orbital participation.

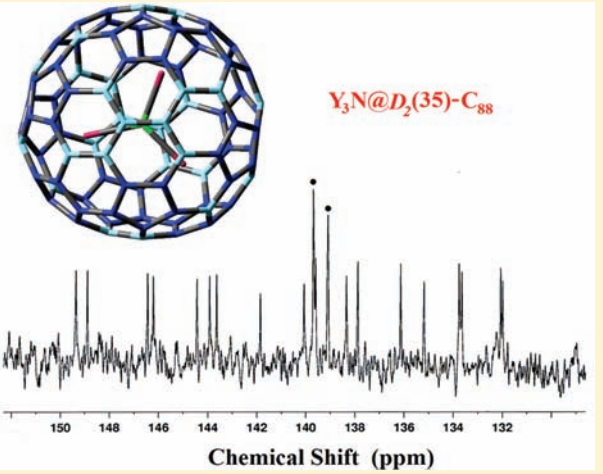

INTRODUCTION

The separation and characterization of higher fullerenes beyond C_{80} is very difficult not only because of their extremely low yield but also because of the possible presence of multiple isomers, instability, and lower solubility.[1] For example, Yang and Dunsch reported the separation of di- and tri-dysprosium endohedral metallofullerenes in the fullerene cages from C_{94} to C_{100}.[2] Because of the limited available amount of sample, they did not obtain any structural information for those large cages.[2] Among the large fullerene cages, the C_{88} cage has been widely studied. As early as 1995, C_{88} empty cage fullerenes were separated from soot generated in a Kratschmer−Huffman electric-arc generator and subsequently characterized using ^{13}C NMR by Achiba et al.[3] In a later report, Miyake et al.[4] described a more detailed ^{13}C NMR study for the C_{88} empty cage fullerene. However, the structural assignments were ambiguous because at least three C_{88} isomers exist.[4] Because of the difficulty in the experimental part, extensive theoretical studies were performed by several groups to aid the structural determination.[5,6] It was predicted that the $C_2(7)$, C_s-(17), and $C_2(33)$ isomers are the mostly likely to be experimentally isolated among the 35 IPR-obeying isomers of C_{88}.[5,6] Derivatization of empty fullerene cages has proven to be an effective tool for cage stabilization and meanwhile provides a path for further structural characterization. For example, Troyanov and Tamm[7] synthesized and characterized trifluoromethyl derivatives of C_{88}, $C_{88}(CF_3)_{18}$. On the basis of their X-ray investigation, they determined that $C_{88}(CF_3)_{18}$ processes a $C_2(33)$-C_{88} cage, which is one of the three most stable isomers predicted on a theoretical basis. Encapsulation of atoms or clusters into fullerene cages is another method used to stabilize empty fullerene cages by electron-transfer processes between the encapsulated and carbon cages.

Trimetallic nitride template (TNT) endohedral metallofullerenes (EMFs) are particularly important not only because of their relatively high yields but also because of their intriguing potential applications in biomedical, optoelectronic, and photovoltaic fields.[8,9] Insertion of a TNT cluster into a C_{88} cage ($A_3N@C_{88}$, where A = Gd, Tm, Dy, Tb, Nd, Pr, Ce, La) has been reported by several laboratories.[10−13] Echegoyen and co-workers suggested that the C_{88} cage is preferentially templated by a TNT cluster for metal ions with ionic radii larger than Gd, such as Nd, Pr, or Ce.[10,11] However, most of the TNT EMFs with the C_{88} cage have been characterized by mass spectroscopy without definitive structural characterization. Notable exceptions are the single-crystal X-ray studies reported for $Tb_3N@C_{88}$, which have been found to have an IPR-obeying $D_2(35)$ structure.[12] This is in contrast with the theoretical predictions for the empty C_{88} cage. Thus, it is interesting to examine whether clusters with different metals $(A_3N)^{6+}$ encapsulated within a C_{88} cage have the same cage structure as IPR-obeying $Tb_3N@D_2(35)$-C_{88}.

In this paper, we report the synthesis, separation, and structural characterization of diamagnetic $Y_3N@C_{88}$. This diamagnetic molecule allows high-resolution ^{13}C NMR structural studies, which are generally not feasible for the paramagnetic lanthanide C_{88} cage TNT EMFs reported above. Density

Received: August 31, 2010
Published: April 20, 2011

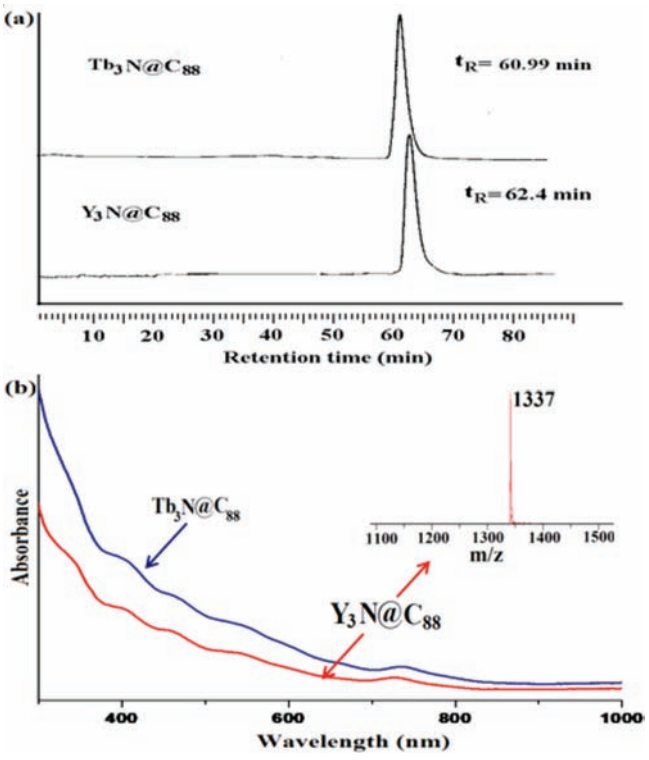

Figure 1. (a) HPLC chromatogram of the purified $Y_3N@C_{88}$ and $Tb_3N@C_{88}$ (10 × 250 mm 5PYE column; λ = 390 nm; flow rate 2.0 mL/min; toluene as the eluent; 25 °C). (b) UV−vis spectra of $Y_3N@C_{88}$ and $Tb_3N@C_{88}$ in toluene and positive-ion LD-TOF MS for purified $Y_3N@C_{88}$.

functional theory (DFT) calculations were utilized to augment the structural determination. The electronic properties of $Y_3N@C_{88}$ were also studied by both electrochemical and DFT computational approaches to compare a nonlanthanide TNT EMF with the corresponding lanthanide TNT EMFs reported to date.

EXPERIMENTAL SECTION

A sample of $Y_3N@C_{88}$ was synthesized in an electric-arc-discharge reactor by vaporizing graphite rods containing a mixture of Y_2O_3 and graphite powder and using Cu as the catalyst with a weight ratio of 1.1:1.0:2.1 in a dynamic flow of N_2 and He (flow rate ratio of N_2:He = 3:100).[14] The toluene extract from the raw soot was applied to a cyclopentadiene-functionalized Merrifield peptide resin. The eluent was further separated by two-stage high-performance liquid chromatography (HPLC). The first stage was carried out on a 5PBB column, and the sixth fraction contains $Y_3N@C_{88}$, which was further purified by a 5PYE column.

The ^{13}C NMR measurements (150 MHz) were performed on a Bruker Advance spectrometer (600 MHz, ^1H). The sample was dissolved in CS_2 with $Cr(acac)_3$ as the relaxation agent and acetone-d_6 as the internal lock at 25 °C. Cyclic voltammetry (CV) was conducted using a CH Instruments 600A potentiostat (Austin, TX) with a single-compartment, three electrode and electrochemical cell. A 2.0 mm glassy carbon working electrode, a platinum wire auxiliary electrode, and a silver wire pseudoreference electrode were used; ferrocene was used as an internal standard.

DFT computations were performed using the *Gaussian 03* program package. All of the molecules were geometrically optimized at the UB3LYP level with a DZVP basis set for yttrium atoms and a 6-31G* basis set for carbon and nitrogen atoms.[14] DFT-optimized energy values

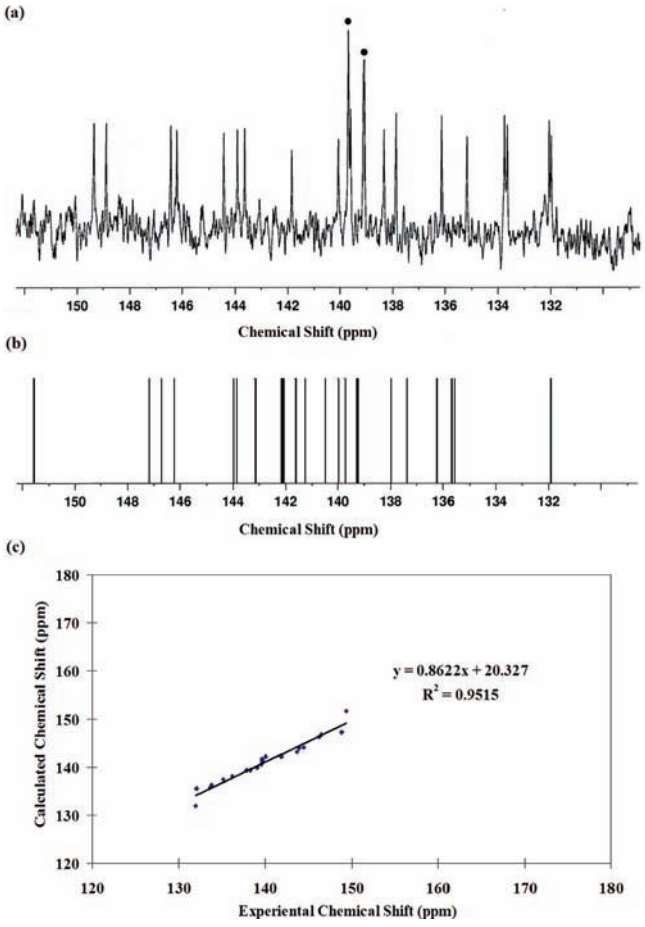

Figure 2. (a) ^{13}C NMR spectrum of $Y_3N@D_2$-C_{88} in CS_2 with 10 mg of $Cr(acac)_3$ relaxant (acetone-d_6 lock) after 64 000 scans at 25 °C, showing the 22 × 4 pattern (number of NMR lines × relative intensity). The symbol • indicate the signals with double intensity. (b) Computational ^{13}C NMR spectrum for $Y_3N@D_2(35)$-C_{88}. The experimental and calculated ^{13}C shifts are provided in the Supporting Information. (c) Correlation between experimental and computational ^{13}C NMR results.

were obtained starting from the X-ray crystallographic structures of the corresponding $Tb_3N@D_2(35)$-C_{88}.[12]

RESULTS AND DISCUSSION

As illustrated in Figure 1, the HPLC, positive-ion laser-desorption time-of-flight mass spectrometry (LD-TOF MS), and UV−vis spectra for $Y_3N@C_{88}$ are compared with data that were previously reported for $Tb_3N@C_{88}$.[12] The close correspondence of the data in Figure 1 strongly suggests that $Y_3N@C_{88}$ has the same $D_2(35)$ cage structure as $Tb_3N@D_2(35)$-C_{88}.[12] Because the $Y_3N@C_{88}$ molecule is diamagnetic, we were able to obtain high-resolution ^{13}C NMR data for $Y_3N@C_{88}$ to further confirm the cage structure.

The ^{13}C NMR spectrum (Figure 2a) for $Y_3N@C_{88}$ exhibits a total of 22 lines (lines at 139.10 and 139.69 ppm, double intensity) with a shift range from 131.0 to 150.0 ppm. An IPR-allowed isomer is suggested because of the absence of a ^{13}C NMR signal above 155 ppm, which is characteristic of non-IPR pentalene motifs.[14] There are 35 IPR-allowed C_{88} isomers and two isomers, (1) and (35), that have D_2 symmetry (22 × 4 lines), which is consistent with the observed spectrum.[15] Among the 35 IPR-obeying isomers for the C_{88} cage, no other IPR-allowed structure exhibits fewer than 22 lines

dx.doi.org/10.1021/ic101772d |*Inorg. Chem.* 2011, 50, 4256–4259

except for isomer (34) with T symmetry, which exhibits eight ^{13}C NMR resonances (1×4 and 7×12). All other C_{88} IPR isomers have lower symmetry and exhibit more than 22 spectral lines. In addition, there are seven pyrene 6,6,6-type carbons that range from 132.0 to 137.9 ppm, which is in reasonably good agreement with seven DFT-predicted values (Figure 2b) ranging from 131.9 to 139.2 ppm.[14] The correlation between the experimental ^{13}C and the DFT-predicted chemical shielding values are shown in Figure 2c. $Tb_3N@D_2(35)$-C_{88} exhibits a carbon cage with D_2 symmetry as determined by previous single-crystal X-ray diffraction studies.

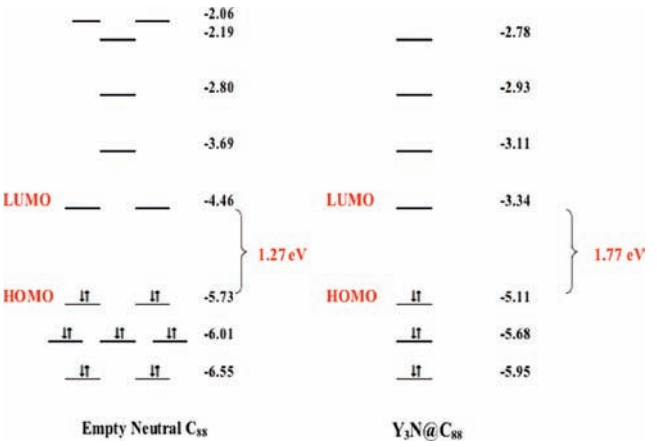

Figure 3. DFT computational HOMO−LUMO levels for the neutral IPR $D_2(35)$-C_{88} and $Y_3N@D_2(35)$-C_{88} cages.

Thus, our current results are consistent with a $Y_3N@D_2(35)$-C_{88} structure in a fashion analogous to that of $Tb_3N@D_2(35)$-C_{88}.[12]

As previously indicated, there are three isomers of empty C_{88} cages, $C_2(7)$, $C_s(17)$, and $C_2(33)$, that are predicted to be thermodynamically and kinetically stable.[5,6] However, C_{88} with $D_2(35)$ symmetry is not included in this group. Computational (DFT) calculations summarized in Figure 3 suggest that the neutral IPR $D_2(35)$-C_{88} has a small HOMO−LUMO gap (1.27 eV), indicating the lower stability of the neutral $D_2(35)$-C_{88} cage. However, upon accepting six electrons, the HOMO−LUMO gap becomes significantly larger (1.77 eV), consistent for the higher stability of the $Y_3N@D_2(35)$-C_{88} molecule. To our knowledge, neither the Y_3N cluster nor the $D_2(35)$-C_{88} cage has been isolated, but when associated together, they form a stable $Y_3N@D_2(35)$-C_{88} structure by electron transfer between the cluster and cage.

As illustrated in Figure 4, the CV electrochemistries of $Y_3N@C_{88}$ and $Gd_3N@C_{88}$ are nearly equivalent. The $Gd_3N@C_{88}$ sample for this CV electrochemistry comparison was isolated and purified (see the Supporting Information) in the same fashion as that described for $Y_3N@C_{88}$ vide supra and is consistent with previously reported data by Echegoyen and co-workers.[16] The electrochemistry of $Y_3N@C_{88}$ and $Gd_3N@C_{88}$ can be described as having two distinct oxidative processes accompanied by first and second reduction peak potentials of −1.43 and −1.70 V, respectively. The redox potentials and resulting electrochemical gap (ΔE_{gap}) for $Y_3N@C_{88}$ are in good agreement with reported literature values for other $M_3N@C_{88}$ systems (Table 1). This is consistent with a single (nondegenerate) LUMO level for $Y_3N@C_{88}$ obtained from the DFT calculations described above. The resulting electrochemical

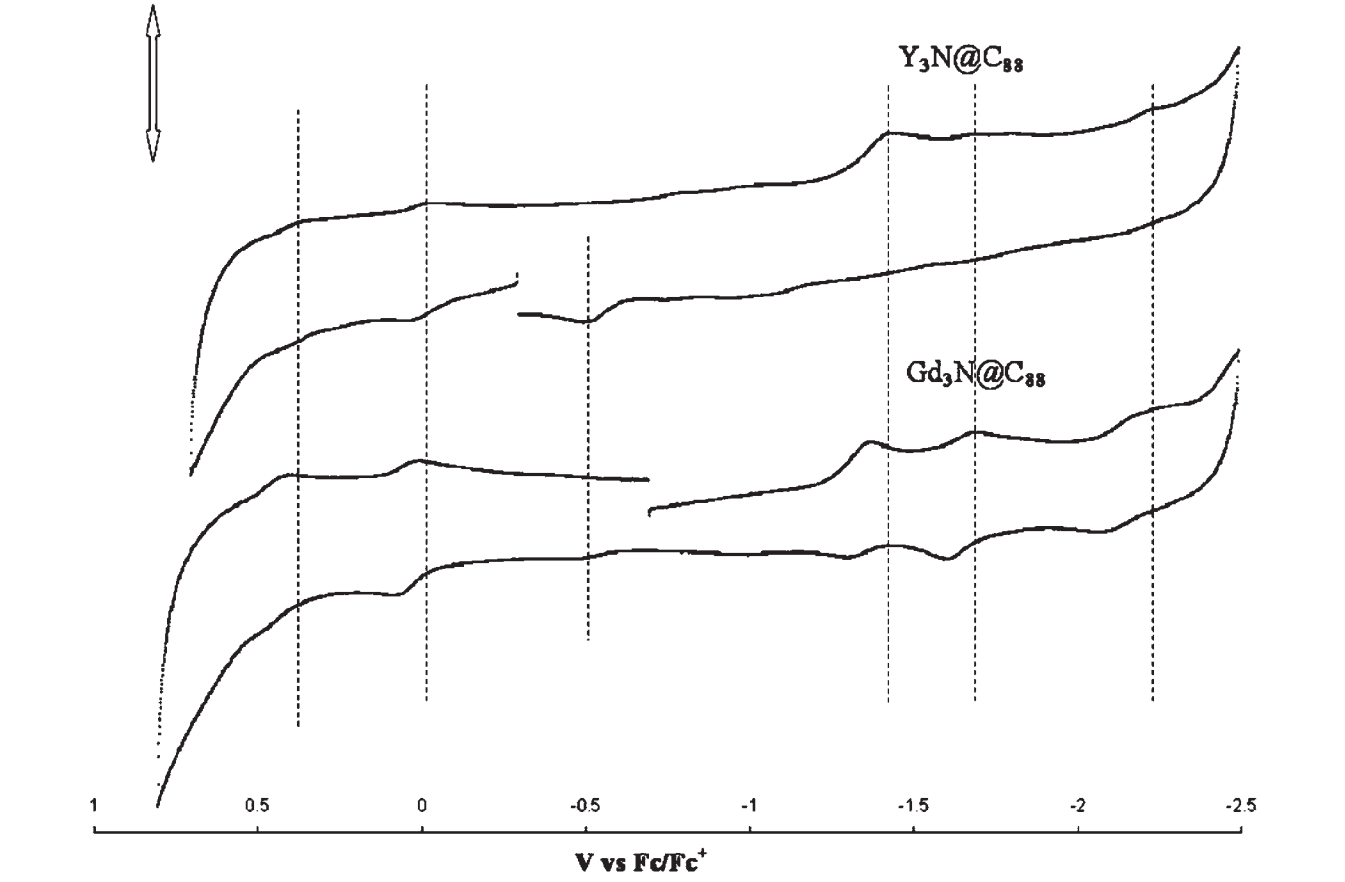

Figure 4. Cyclic voltammogram of $Y_3N@C_{88}$ and $Gd_3N@C_{88}$; 100 mV/s; 0.1 M $TBABF_4$ in o-DCB.

dx.doi.org/10.1021/ic101772d |Inorg. Chem. 2011, 50, 4256–4259

Table 1. Redox Potential of the $A_3@C_{2n}$ Endohedral Metallofullerenes

	$E_{1/2}^{ox1}$	$E_{1/2}^{ox2}$	E_{pc}^{red1}	E_{pc}^{red2}	ΔE_{gap}
$Y_3N@I_h$-C_{80}[15]	0.64		−1.41	−1.83	2.05
$Y_3N@C_{88}$	0.03	0.43	−1.43	−1.70	1.46
$Gd_3N@C_{88}$	0.05	0.45	−1.39	−1.71	1.44
$Gd_3N@C_{88}$[16]	0.06	0.49	−1.43	−1.74	1.49
$Nd_3N@C_{88}$[10]	0.07	0.53	−1.36	−1.75	1.43
$Pr_3N@C_{88}$[9]	0.09	0.54	−1.34	−1.72	1.43
$Ce_3N@C_{88}$[9]	0.08	0.63	−1.30	−1.57	1.38
$La_3N@C_{88}$[9]	0.21	0.66	−1.34	−1.67	1.57

band gap $^{ox}E_1 - {}^{red}E_1$ for $Y_3N@C_{88}$ is 1.46 V, reasonably consistent with the DFT predictions above. Although $^{ox}E_1 - {}^{red}E_1$ for $Y_3N@C_{88}$ is smaller than that for the more stable $Y_3N@C_{80}$ case,[16] this band gap is similar to other $M_3N@C_{88}$ family members, such as $Gd_3N@C_{88}$ (1.49 V),[17] $Nd_3N@C_{88}$ (1.43 V),[11] $Pr_3N@C_{88}$ (1.43 V),[9] $Ce_3N@C_{88}$(1.38 V),[9] and $La_3N@C_{88}$(1.57 V).[9] These results suggests that the $^{ox}E_1 - {}^{red}E_1$ band gap (and corresponding HOMO−LUMO gap) of $A_3N@C_{88}$ trimetallic nitride endohedral metallofullerenes is a property dominated by the properties of the $D_2(35)$-C_{88} carbon cage and not the nature of the yttrium or lanthanide electronic metal cluster $(A_3N)^{6+}$.

CONCLUSION

In summary, we have synthesized, purified, and characterized diamagnetic $Y_3N@C_{88}$ for the first time. The ^{13}C NMR study indicates that $Y_3N@C_{88}$ exhibits an IPR-obeying $D_2(35)$-C_{88} cage. The electrochemical data suggested that $Y_3N@C_{88}$ has a smaller HOMO−LUMO gap than $Y_3N@C_{80}$, which is consistent with the computational DFT study. Also, our results show that encapsulation of an Y_3N cluster does not significantly alter the electrochemical properties of these trimetallic nitride endohedral metallofullerenes, and this result is consistent with other lanthanide M_3N clusters in $D_2(35)$-C_{88} cages. This suggests that the unique $D_2(35)$-C_{88} cage properties strongly influence the electrochemical and electronic properties of these trimetallic nitride endohedral metallofullerenes.

ASSOCIATED CONTENT

Supporting Information. Extra information for Figure 2, an HPLC chromatogram, a table of components and yields, and LD-TOF MS spectra. This material is available free of charge via the Internet at http://pubs.acs.org.

NOTE ADDED IN PROOF

Recently, a study of Lu3N@C_{88} was reported.[18]

AUTHOR INFORMATION

Corresponding Author

*E-mail: hdorn@vt.edu. Tel: 540-231-5953. Fax: 540-231-3255.

ACKNOWLEDGMENT

We gratefully acknowledge support by the National Science Foundation [Grants CHE-0443850 and DMR-0507083 (to H.C. D.)] and the National Institutes of Health [Grant 1R01-CA119371-01 (to H.C.D.)]. We also acknowledge Dr. Jiechao Ge for his help with some of the preparation for this work.

REFERENCES

(1) Popov, A. A.; Dunsch, L. *J. Am. Chem. Soc.* **2007**, *129*, 11835–11849.
(2) Yang, S.; Dunsch, L. *Angew. Chem., Int. Ed.* **2006**, *45*, 1299–1302.
(3) Achiba, Y.; Kikuchi, K.; Aihara, Y.; Wakabayashi,T.; Miyake, Y.; Kainosho, M. In *Science and Technology of Fullerene Materials*; Bernier P., Bethune, D. S., Chiang, L. Y., Ebbesen, T. W., Metzger, R. M., Mintmire, J. W., Eds.; MRS Symposia Proceedings No. 359; Material Reasearch Society: Pittsburgh, PA, 1995; pp 3−9.
(4) Miyake, Y.; Minami, T.; Kikuchi, K.; Kainosho, M.; Achiba, Y. *Mol. Cryst. Liq. Cryst.* **2000**, *340*, 553–558.
(5) Watanabe, M.; Ishimaru, D.; Mizorogi, N.; Kiuchi, M.; Aihara, J. I. *THEOCHEM* **2005**, *726*, 11–16.
(6) Sun, G. Y. *Chem. Phys. Lett.* **2003**, *367*, 26–33.
(7) Troyanova, S.; Tamm, N. B. *Chem. Commun.* **2009**, 6035–6037.
(8) Fatouros, P. P.; Corwin, F. D.; Chen, Z. J.; Broaddus, W. C.; Tatum, J. L.; Kettenmann, B.; Ge, Z. X.; Gibson, H. W.; Russ, J. L.; Leonard, A. P.; Duchamp, J. C.; Dorn, H. C. *Radiology* **2006**, *240*, 756–764.
(9) Ross, R. B.; Cardona, C. M.; Guldi, D. M.; Sankaranarayanan, S. G.; Reese, M. O.; Kopidakis, N.; Peet, J.; Walker, B.; Bazan, G. C.; Van Keuren, E.; Holloway, B. C.; Drees, M. *Nat. Mater.* **2009**, *8*, 208–212.
(10) Chaur, M. N.; Melin, F.; Elliott, B.; Kumbhar, A.; Athans, A. J.; Echegoyen, L. *Chem.—Eur. J.* **2008**, *14*, 4594–4599.
(11) Melin, F.; Chaur, M. N.; Engmann, S.; Elliott, B.; Kumbhar, A.; Athans, A. J.; Echegoyen, L. *Angew. Chem., Int. Ed.* **2007**, *46*, 9032–9035.
(12) Zuo, T. M.; Beavers, C. M.; Duchamp, J. C.; Campbell, A.; Dorn, H. C.; Olmstead, M. M.; Balch, A. L. *J. Am. Chem. Soc.* **2007**, *129*, 2035–2043.
(13) Yang, S. F.; Dunsch, L. *J. Phys. Chem. B* **2005**, *109*, 12320–12328.
(14) Fu, W. J.; Xu, L. S.; Azurmendi, H.; Ge, J. C.; Fuhrer, T.; Zuo, T. M.; Reid, J.; Shu, C. Y.; Harich, K.; Dorn, H. C. *J. Am. Chem. Soc.* **2009**, *131*, 11762–11769.
(15) Fowler, P. W. Manolopoulos, D. E. *An Atlas of Fullerenes*; Clarendon Press: Oxford, U.K., 1995.
(16) Cardona, C. M.; Elliott, B.; Echegoyen, L. *J. Am. Chem. Soc.* **2006**, *128*, 6480–6485.
(17) Charu, M. N.; Melin, F.; Elliott, B.; Athans, A. J.; Walker, K.; Holloway, B. C.; Echegoyen, L. *J. Am. Chem. Soc.* **2007**, *129*, 14826–14829.
(18) Xu, W.; Wang, T. S.; Wu, J.-Y.; Ma, Y.-H.; Zheng, J.-P.; Li, H.; Wang, B.; Jiang, L.; Shu, C.-Y.; Wang, C. R. *J. Phys. Chem. C* **2011**, *115* (2), 402–405.